Journal of Sol-Gel Science and Technology 32, 173–177, 2004

Hybrid Inorganic-Organic Sol–Gel Coatings in the SiO_2-TiO_2 System

MARIA ZAHARESCU,* MARIA CRISAN, LUMINITA PREDOANA AND MARIUCA GARTNER,
Institute of Physical Chemistry, Romanian Academy, 202 Splaiul Independentei, 060021 Bucharest, Romania
mzaharescu@icf.ro

DANA CRISTEA, STEFANIA DEGERATU AND ELENA MANEA
National Institute for R&D in Microtechnologies, P.O. Box 36-160, Bucharest, Romania

Abstract. In the present work, the influence of substituted Si-alkoxides on the structural and optical properties of films obtained in the SiO_2-TiO_2 system was studied. Methyltriethoxysilane (MTEOS) and 3-(tri-methoxysilyl)propyl methacrylate (TSPM) were used as SiO_2 sources and $Ti(OBu)_4$ was used as TiO_2 source. Acetylacetone was added to the $Ti(OBu)_4$ as chelating agent and the synthesis was carried out in acid medium. The films were deposited on oxidized Si-wafers by spin-coating. The films were characterized by XRD, spectro-ellipsometry (SE), and atomic force microscopy (AFM). The results obtained have shown that in the case of hybrid films the desired thickness could be obtained in a single deposition step. The thickness of the films and the optical properties are controlled by the bulkiness of the organic substitute bounded to Si. Among other optical applications, the potential use of such films as optical waveguides is proposed.

Keywords: hybrid sol–gel films, SiO_2-TiO_2 system, waveguides

1. Introduction

The sol–gel process, with its intrinsically low processing temperatures, allows the incorporation of organic moieties within inorganic networks, leading to the formation of organic-inorganic hybrid materials. Such hybrid materials can offer multifunctionality and allow properties to be tailored from subnanometer (near-atomic) to submicron (mesoscopic) length scales. The organic groups can modify the inorganic backbone by reducing the connectivity of the gel network, allowing thick film deposition and lowering of the processing temperature. These films could play a significant role in the field of micro- and nano-photonic devices (waveguides, emitting devices, quantum dot devices, photonic band gaps and holographic materials).

In spite of the fact that the study of waveguides started many years ago on inorganic systems, the first hybrid inorganic-organic waveguides, obtained by the sol–gel method, were reported by Krug et al. [1] and by Najafi and Sanchez [2, 3]. In the last few years, hybrid waveguides obtained from methacryloxypropyltrimethoxysilane (MEMO) and $Zr(OPr)_4$ were investigated [4–6] and new films for integrated optics based on organic modified silica were developed [7–9].

It is well known that sol–gel films in the SiO_2-TiO_2 system are suitable for a variety of optical applications, due to the high refractive index of TiO_2 that enables the refractive index of coatings to be controlled by varying the amount of TiO_2 in the composition. As compared with the similar pure oxide compositions, in the case of the sol–gel hybrid inorganic-organic compositions, monolayer films with desired thickness can also be obtained. SiO_2-TiO_2 coatings with a thickness of 2 μm, made by single step dip coating, were prepared as planar waveguides by Brusatin et al. [10], using acid catalysed solutions of methyltriethoxysilane (MTEOS) mixed with tetraethoxysilane (TEOS) and

*To whom all correspondence should be addressed.

tetrabutoxytitanate as precursors. Inorganic and hybrid organic-inorganic silica (SiO_2)-titania (TiO_2) planar waveguides, with a relative molar composition of 70–30, have been fabricated by Innocenzi et al. [11] via dip coating.

In one of our previous studies [12], sol–gel oxide films with special optical properties in the SiO_2-TiO_2 system were obtained. A systematic study of the sol–gel process in model systems based on tetraethoxysilane (TEOS), methyltriethoxysilane (MTEOS) and vinyltriethoxysilane (VTEOS) was also undertaken [13] and the results were discussed in comparison with a more complex system prepared using phenyltriethoxysilane (PTEOS) and methacryloxypropyltrimethoxysilane (MEMO) [14].

In the present work, a study of the influence of substituted Si-alkoxides on the structural and optical properties of hybrid films obtained in the SiO_2-TiO_2 system, using methyltriethoxysilane (MTEOS) and 3-(tri-methoxysilyl)propyl methacrylate (TSPM) as SiO_2 sources, and $Ti(OBu)_4$ as TiO_2 source is reported.

2. Experimental

2.1. Film Preparation

Two reaction mixtures, with different alkoxide precursors as SiO_2 source, namely methyltriethoxysilane (MTEOS) and 3-trimethoxysilylpropylmethacrylate (TSPM), were synthesized that correspond to molar composition (mol%): $70SiO_2$-$30TiO_2$. Tetrabutoxyorthotitanate, $Ti(OBu^t)_4$, was used as the TiO_2 source. The composition of the initial solutions (molar ratios) and the experimental conditions used are presented in Table 1. An equivalent oxide concentration of wt% was used for both precursor solutions.

In order to avoid the tendency for titania phase separation or precipitation during the sol–gel process, AcAc was used as a chelating agent. The molar ratio $AcAc/Ti(OBu)_4 = 0.05$–0.5. The compositions were selected from the paper [11].

2.2. Film Deposition

Supported films on SiO_2 (300 nm)/silicon wafer substrates were obtained by spin-coating (2000 rpm), using the solutions presented in Table 1. Before deposition, the solutions were aged for 24 h. The films were heated at 100°C for 1 h, using a heating rate of 1°C/min.

2.3. Film Characterization

The optical properties of the SiO_2-TiO_2 hybrid films were determined by spectroellipsometry (SE) measurements in the visible range (0.4–0.7 μm). The modelling of the experimental ellipsometric spectra was made with the multilayer and multicomponent Bruggemann's effective medium approximation (BEMA) model. The thickness and the volume fraction of the components (R-SiO_2, TiO_2 for hybrid films; and SiO_2, TiO_2 for oxide films) were used as fit parameters. Optical bandgaps were calculated using the *Wemple Di Domenico* model [15]:

$$n^2(\omega) - 1 \cong \frac{E_d E_0}{\left(E_0^2 - E^2\right)}$$

where E_d is the dispersion energy, which measures the average strength of the interband optical transitions (associated with changes in the structural order of the material) and E_0 is the oscillation energy, which can be correlated with the optical gap by empirical formula [16]:

$$E_0 = 1.7E_g$$

Structural characterization was undertaken with XRD (TuR M-62 with HZG-3 equipment), and the morphology of the films was investigated by scanning electron microscopy (SEM; AMR MODEL 1000 equipment).

3. Results and Discussion

With the conditions used, continuous and homogeneous films, with good adherence to the substrates were

Table 1. Composition of the initial solution and experimental conditions used for preparation of the hybrid films in the SiO_2-TiO_2 system.

		Molar ratio				Reaction conditions	
Sample	Precursors	ROH: Σ(precursor)	H_2O: Σ(precursor)	H^+: Σ(precursor)	pH	T (°C)	T (hrs)
A	MTEOS: $Ti(OBu^t)_4 = 2.33$, AcAc	11.34	1.4	0.097	4	20	2 in air
B	TSPM: $Ti(OBu^t)_4 = 2.50$, AcAc	2.3	1.25	0.071	3	20	2 in air

Table 2. Thickness and volume fractions of the components obtained from ellipsometric measurements (SE) together with thickness from SEM.

Type of film	Precursors	T (°C)	d_{SEM}(nm)	d_{SE} (nm)	R-SiO_2 (%)	SiO_2 (%)	TiO_2 (%)	E_g (eV)
Hybrid	MTEOS + $Ti(OBu)_4$	20	–	294	70.1		29.9	4.09
Hybrid	MTEOS + $Ti(OBu)_4$	100	214	285	70.5	–	29.5	4.11
Hybrid	TSPM + $Ti(OBu)_4$	100	2670	–	–	–	–	–
Oxide [12]	TEOS + $Ti(OBu)_4$	300	–	98	–	69.9	30.1	4.30

obtained. XRD results have demonstrated the amorphous character of the initial and thermally treated (1 h 100°C) coatings. The optical properties of the films determined by SE measurements are presented in Table 2 and Fig. 1(a) and (b). It can be observed that the refractive index (n) of the oxide films is higher than that of the hybrid films (due to the lower refractive index of the organic components), while the optical band gap exhibits a similar trend.

In Table 2, the thickness and volume fractions of the components obtained from ellipsometric measurements, together with the thickness obtained from SEM determination (d_{SEM}) for the samples thermally treated at 100°C, are presented. SEM images of the films are shown in Fig. 2. For comparison, the results obtained starting with un-substituted Si-alkoxides are also presented in Table 2. More details on the preparation and characterization of the oxide films are presented in a previous paper [12].

The hybrid film with SiO_2-TiO_2 inorganic network obtained from MTEOS has a much higher thickness then the corresponding pure oxide films. The apparent thicknesses measured by spectroellipsometry and SEM are in relatively good agreement. Due to the very high thickness of the films obtained with TSPM, the ellipsometric determinations were not relevant, due to

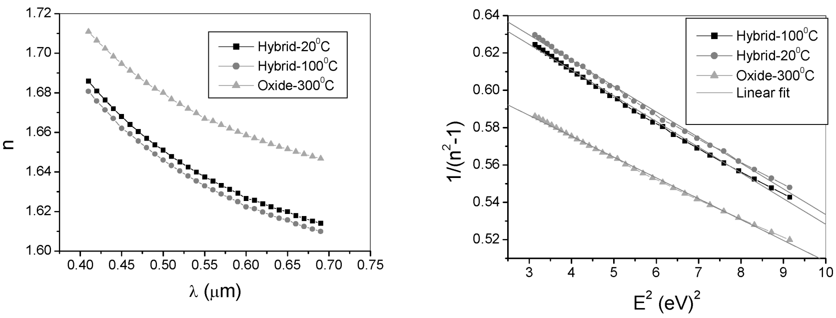

(a) (b)

Figure 1. (a) The dispersion of the refractive indices of the films. (b) Fits obtained using the *Wemple DiDomenico* model.

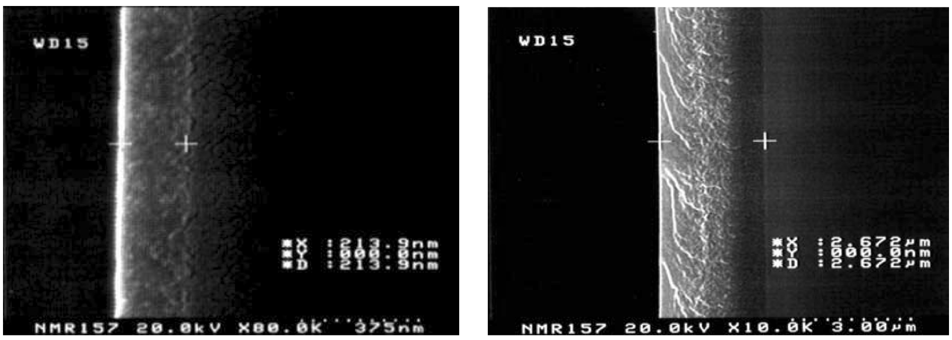

A B

Figure 2. SEM images of the cross section of the films prepared with (A) MTEOS + $Ti(OBu)_4$, and (B) TSPM + $Ti(OBu)_4$.

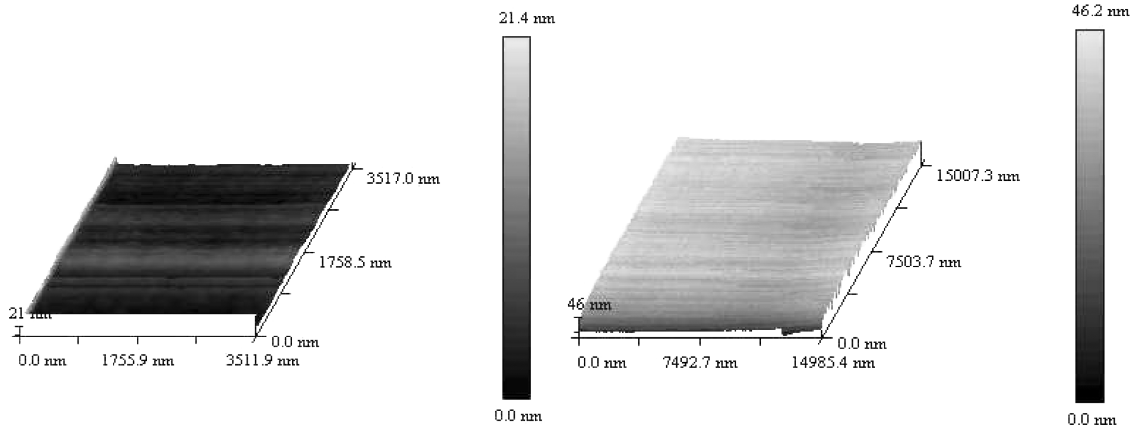

A O

Figure 3. AFM images of single-layer thermally treated hybrid film prepared with MTEOS + $Ti(OBu)_4$ (A), and SiO_2-TiO_2 oxide films (O).

the fact that the method is only suitable for thin films characterization (i.e. below 1 μm). However, from the SEM results presented in Fig. 2, one may observe that the type of organic radical chemically bonded to the Si influences the thickness of the film obtained, depending on their bulkiness (note that all other coating parameters were maintained essentially constant). One can see that the thickness of the films starting with TSPM is very high (>2.6 μm) while the film obtained starting with MTEOS has a thickness of only about 200–300 nm.

After the thermal annealing at 100°C, the hybrid samples undergo only small changes in thickness and refractive index, while as expected, oxide sample thermally treated at 300°C exhibit a significant decrease in their thickness due to densification [12].

The SEM images of the cross section of the films show dense morphology and a very smooth surface in both cases (Fig. 2(A) and (B)).

The AFM images (Fig. 3) obtained from the oxide and hybrid films (MTEOS system) revealed a smooth, featureless surface topology as expected for homogeneous, amorphous materials (consistent with the XRD data). Over the length scales used in Fig. 3, the samples exhibited low roughness, ranging from 2 to 6 nm, depending on the film composition.

4. Applications

Waveguides with a sol–gel core could be obtained by patterning the sol–gel layer using a photoresist mask. The sol–gel layer was deposited by spinning on oxidized silicon wafers ($x_{ox} = 300$ nm). The thickness of the sol gel layer was 213 nm for MTEOS + $Ti(OBu)_4$ and 2.67 μm for the TSPM + $Ti(OBu)_4$ composition. The etching was performed in a HF:CH_3COOH (1:2) solution, for 20–30 min. The films obtained are

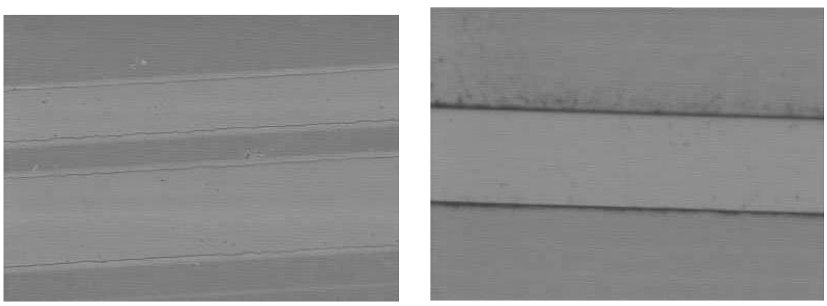

A B

Figure 4. Waveguides obtained by pattering films obtained starting with (A) MTEOS + $Ti(OBu)_4$, and (B) TSPM + $Ti(OBu)_4$.

illustrated in Fig. 4. Due to the presence of the organic component, the etching process is much slower that in the case of pure oxide layers and the lateral walls obtained are not as straight. To improve the quality of the lateral walls, plasma etching could be used.

In future work, the waveguides will be integrated and coupled to silicon photodiodes to measure the attenuation and to fabricate photonic circuits for optical communications.

5. Conclusions

The results obtained in this work, which investigated the effect of selected organic modifiers (methyl and propylmethacrylate) on the optical and structural properties of organically modified SiO_2/TiO_2 hybrids, emphasize the possibilities offered by sol–gel processing to design and process films with tailored properties both in oxide and hybrid inorganic-organic systems. Structure and properties of the films were determined by XRD, spectroellipsometry, SEM and AFM methods. As compared to the corresponding pure oxide compositions, the hybrid films exhibit suitable thickness in a single deposition step for applications such as waveguiding. Patterning of the films, using suitable photoresist masks and etching in HF:CH_3COOH solutions, indicated that structures with dimensions potentially suitable for waveguiding applications could be produced. Future work will investigate the use of these patterned coatings in photonic circuits for optical communications.

Acknowledgment

The work was realized in the frame of MATNANTECH project, contract no. 86a/2001. One of the authors (M.Gartner) wishes to acknowledge the support of the EU Transactional Access Programme, under the RIMDAC scheme at the NMRC, University College Cork, IRELAND for the SEM micrographs.

References

1. H. Krug, F. Tiefenesee, P.W. Oliveira, and H. Schmidt, S.P.I.E. Sol-Gel Optics II **1758**, 448 (1992).
2. S.I. Najafi, C.Y. Li, M. Andrews, J. Chisham, and P. Lefebvre, *Confernce on Functional Photonic Integrated Circuits* (San Jose, SPIE Proc., 1995), vol. 2041, p. 110.
3. C. Sanchez and F. Ribot, New J. Chem. **18**, 1007 (1994).
4. S.I. Najafi, T. Touam, R. Sara, M.P. Andrews, and M.A. Fardad, J. Lightwave Technol. **16**, 1640 (1998).
5. E. Giorgetti, G. Margheri, S. Sottini, M. Casalboni, R. Senesi, M. Scarselli, and R. Pizzoferrato, J. Non-Cryst. Solids **255**, 193 (1999).
6. Y. Moreau, K. Kribich, P. Courdray, P. Etienne, and J. Galy, *Int. Conf. SPIE: Photonics West*, January 2002 (San Jose, USA, 2002), vol. OE-4640, p. 60.
7. R. Corriu and D. Leclerd, Angew. Chem. **108**, 1524 (1996).
8. O.S. Rösch, W. Bernhard, R. Müler-Fiedler, P. Danberg, A. Bräuer, R. Buestrich, and M. Popall, *S.P.I.E., Conference on Linear Optical Properties of Waveguides and Fibers* (Denver, Colorado, 1999), vol. 3799, p. 214.
9. R. Buetrich, F. Kahlenberg, M. Popall, P. Dannberg, R. Muler-Fiedler, and O. Rosch, J. Sol–Gel Sci. Technol. **20**, 181 (2001).
10. G. Brusatin, M. Guglielmi, P. Innocenzi, A. Martucci, G.C. Battaglin, S. Pelli, and G.C. Righini, J. Non-Cryst. Solids **220**, 202 (1997).
11. P. Innocenzi, A. Martucci, M. Guglielmi, L. Armelao, S. Pelli, G.C. Righini, and G.C. Battaglin, J. Non-Cryst. Solids **259**, 182 (1999).
12. M. Crisan, M. Gartner, M. Zaharescu, L. Predoana, D. Cristea, E. Manea, and M. Caldararu, *Proceedings of the 10th IEEE Int. Symposium on Electron Devices for Microwave and Optoelectronic Applications (EDMO 2002)* (Manchester, UK, 2002), p. 205.
13. A. Jitianu, A. Britchi, C. Deleanu, V. Badescu, and M. Zaharescu, J. Non-Cryst. Solids **319**, 263 (2003).
14. A. Jitianu, M. Gartner, M. Zaharescu, D. Cristea, and E. Manea, Mat. Sci. Eng. C **23**, 301 (2003).
15. S.H. Wemple and M. DiDomenico, Phys. Rev. **B3**(4), 1338 (1971).
16. I. Solomon, M.P. Schmidt, C. Senemaud, and M. Dreiss Khodja, Phys. Rev. B38(18), 13263 (1988).